AIP | The Journal of Chemical Physics

Communication: Orientational self-ordering of spin-labeled cholesterol analogs in lipid bilayers in diluted conditions

Maria E. Kardash and Sergei A. Dzuba

Citation: The Journal of Chemical Physics **141**, 211101 (2014); doi: 10.1063/1.4902897
View online: http://dx.doi.org/10.1063/1.4902897
View Table of Contents: http://scitation.aip.org/content/aip/journal/jcp/141/21?ver=pdfcov
Published by the AIP Publishing

Communication: Orientational self-ordering of spin-labeled cholesterol analogs in lipid bilayers in diluted conditions

Maria E. Kardash and Sergei A. Dzuba[a)]
Voevodsky Institute of Chemical Kinetics and Combustion, 630090 Novosibirsk, Russia, and Novosibirsk State University, 630090 Novosibirsk, Russia

(Received 13 October 2014; accepted 17 November 2014; published online 1 December 2014)

Lipid-cholesterol interactions are responsible for different properties of biological membranes including those determining formation in the membrane of spatial inhomogeneities (lipid rafts). To get new information on these interactions, electron spin echo (ESE) spectroscopy, which is a pulsed version of electron paramagnetic resonance (EPR), was applied to study 3β-doxyl-5α-cholestane (DCh), a spin-labeled analog of cholesterol, in phospholipid bilayer consisted of equimolecular mixture of 1,2-dipalmitoyl-*sn*-glycero-3-phosphocholine and 1,2-dioleoyl-*sn*-glycero-3-phosphocholine. DCh concentration in the bilayer was between 0.1 mol.% and 4 mol.%. For comparison, a reference system containing a spin-labeled 5-doxyl-stearic acid (5-DSA) instead of DCh was studied as well. The effects of "instantaneous diffusion" in ESE decay and in echo-detected (ED) EPR spectra were explored for both systems. The reference system showed good agreement with the theoretical prediction for the model of spin labels of randomly distributed orientations, but the DCh system demonstrated remarkably smaller effects. The results were explained by assuming that neighboring DCh molecules are oriented in a correlative way. However, this correlation does not imply the formation of clusters of cholesterol molecules, because conventional continuous wave EPR spectra did not show the typical broadening due to aggregation of spin labels and the observed ESE decay was not faster than in the reference system. So the obtained data evidence that cholesterol molecules at low concentrations in biological membranes can interact via large distances of several nanometers which results in their orientational self-ordering. © *2014 AIP Publishing LLC*. [http://dx.doi.org/10.1063/1.4902897]

INTRODUCTION

It is assumed generally that structural organization of biological membranes may be heterogeneous, containing lateral nanodomains (lipid rafts) which are enriched in cholesterol and saturated lipids.[1–5] These nanodomains may serve as platforms for functioning membrane proteins. To get insight into the mechanisms of raft formation, it is necessary to study properties of lipid-cholesterol interactions.

Cholesterol is present in cell membranes at high concentrations of typically around 20–30 mol.% or more. However, information obtained in more diluted conditions could highlight the nature of the long-range cholesterol-cholesterol interactions, which may be important for understanding and modeling different structural and dynamical properties of biological membranes. Here, we report data on the self-ordering of the spin-labeled cholesterol analog 3β-doxyl-5α-cholestane (DCh) presented in lipid bilayers at concentrations in the range of 0.1–4 mol.%.

We employ bilayers prepared from equimolecular mixture of 1,2-dipalmitoyl-*sn*-glycero-3-phosphocholine (DPPC) and 1,2-dioleoyl-*sn*-glycero-3-phosphocholine (DOPC), that is often used as a model for the outer leaflet of the animal cell plasma membrane.[6] For comparison, a reference system containing a spin-labeled 5-doxyl-stearic acid (5-DSA) instead of DCh was studied as well. Electron spin echo (ESE) spectroscopy, a pulsed version of electron paramagnetic resonance (EPR),[7] was employed as an experimental tool. The ESE approach used was based on a mechanism called "instantaneous diffusion" in ESE signal dephasing.[8]

a)Author to whom correspondence should be addressed. Electronic mail: dzuba@kinetics.nsc.ru, Fax: +7(383) 330 7350.

"Instantaneous diffusion" mechanism in ESE decay

The phenomenon of "instantaneous diffusion" arises in electron spin echo because of the sudden modulation by microwave pulses of the magnetic dipole-dipolar interactions between neighboring electron spins. For a uniform spatial distribution of spins, in a two-pulse Hahn echo experiment the echo signal amplitude taken at the position B_0 of the external magnetic field and at the time separation τ between pulses, $E(2\tau, B_0)$, decays with increasing τ due to this phenomenon as follows:[7,9]

$$E(2\tau, B_0) = E(0, B_0)\exp\left(-2\tau\frac{4\pi^2}{9\sqrt{3}}\gamma^2\hbar C\kappa \times\left\langle \sin^2\tfrac{1}{2}\xi_{(B_0-B)}\right\rangle_{g(B)}\right), \quad (1)$$

where γ is the electron gyromagnetic ratio, C is the local spin concentration (measured in cm^{-3} units), κ is the dimensionless correction coefficient (see below), $\xi_{(B_0-B)}$ is the turning angle of the magnetization at the field position B by the second microwave pulse, and $\langle\ldots\rangle_{g(B)}$ denotes averaging over the EPR spectral density $g(B)$ (that is, the EPR lineshape). The factor $\langle\sin^2\frac{1}{2}\xi_{(B_0-B)}\rangle_{g(B)}$ for an ideal rectangular microwave

pulse is given by[9]

$$\langle \sin^2 \tfrac{1}{2}\xi_{(B_0-B)}\rangle_{g(B)} = \frac{\int g(B)dB \frac{B_1^2}{(B_0-B)^2+B_1^2} \sin^2\left(\frac{\gamma t_p}{2}\sqrt{(B_0-B)^2+B_1^2}\right)}{\int g(B)dB}, \quad (2)$$

where B_1 and t_p are the second microwave pulse amplitude and duration, respectively. The dimensionless correction coefficient, $\kappa < 1$, reflects mainly the non-ideality of the microwave pulse shape and also partial destruction of the instantaneous diffusion effect by electron spin-lattice relaxation.[9] Note that in EPR, the pulse excitation bandwidth is normally much less than the total linewidth.

The optimal conditions to observe the effect of instantaneous diffusion are attained by setting $\gamma t_p B_1 = \pi$. One can estimate from Eq. (1) that, for $\tau \sim 10^{-6}$ s, which is typical for ESE experiments on organic solids (the transverse relaxation time T_2 is of that order), and for the most optimal cases of $\langle \sin^2 \frac{1}{2}\xi_{(B_0-B)}\rangle_{g(B)} \sim 1$ and $\kappa \sim 1$, the decay will be observed for a local spin concentration C as small as $\sim 10^{18}$ cm^{-3} (corresponding to the inter-spin distances as large as 10 nm). For phospholipid membranes, this concentration corresponds to ~ 0.1 mol.%.

The effect of instantaneous diffusion was employed to measure local concentrations of free radicals appearing in irradiated solids,[10–12] and was observed in different other applications, including studies of spin labels in biological systems,[13,14] transition metal ions in solids,[15] phosphorus donors in silicon.[16,17]

The echo decay with increasing τ is induced by also spin relaxation of electrons and nuclei, and it depends on the electron spin concentration (due to relaxation of electron spins). However, the contribution of instantaneous diffusion can be easily extracted from the total echo decay because of its dependence on $\langle \sin^2 \frac{1}{2}\xi_{(B_0-B)}\rangle_{g(B)}$.

EXPERIMENTAL

Phosphatidylcholines DPPC and DOPC along with spin-labeled cholesterol analog DCh were obtained from Avanti Polar Lipids (Birmingham, AL). 5-DSA was obtained from Sigma-Aldrich. The chemical structures of cholesterol (given here for comparison), DCh and 5-DSA are provided below:

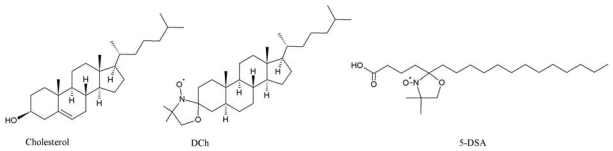

The lipids DPPC and DOPC were co-dissolved in chloroform at a proportion of 1:1 w/w, with DCh or 5-DSA added at different concentrations between 0.1 and 4 mol.%. The solvent was removed by nitrogen flow followed by storage for 12 h under vacuum (10^{-2} bar). The obtained samples were hydrated for 2 h at room temperature by adding bidistilled water at a lipid/water ratio of 1:4 w/w, which resulted in the formation of large multilamellar vesicles. The samples were put into glass tubes of 3-mm outer diameter and frozen by immersion in liquid nitrogen.

A Bruker ELEXSYS E580 9-GHz FT-EPR spectrometer (Bruker, Germany) was used, equipped with either a split-ring resonator (Bruker ER 4118X-MS3) or a dielectric resonator (Bruker ER 4118X-MD5) inside an Oxford Instruments CF 935 cryostat. The split-ring resonator was used in pulsed experiments, while the dielectric resonator – in continuous wave (CW) experiments. The incident microwave power in CW experiments was controlled to ensure the absence of saturation of the EPR spectra. In pulse experiments, the resonator was overcoupled to provide a short ring time (~100 ns). A two-pulse ESE sequence was employed (16-*ns pulse* - τ - 32-*ns pulse* - τ - *echo*). The pulse amplitudes were adjusted to provide turning angles of $\pi/2$ and π for the first and second pulses. To acquire ESE decay time traces, the time delay τ was scanned with a step of 4 ns.

All data processing was performed on a PC using home-made programs. The cryostat was cooled by flowing cold nitrogen gas. The sample temperature was controlled with an accuracy of ±0.5 K.

RESULTS

The obtained conventional CW EPR spectra (data not given) taken at room temperature at low spin label concentrations were similar for those reported in the literature for 5-DSA[18] and DCh[18–20] incorporated into membranes; at low temperatures spectra were typical for immobilized EPR nitroxides. With increasing the spin label concentrations, a slight EPR line broadening was observed that was typical for EPR spectra known for concentrated spin labels in ordered molecular arrays.[21]

All ESE measurements were performed at 77 K. Two kinds of experiments were done. The first one was measurement of echo field dependencies with a scanning magnetic field and fixed τ (so-called echo-detected (ED) EPR spectra). These data are shown in Fig. 1 for DCh (a) and 5-DSA (b), for concentration of 2 mol.% in both cases. For convenience, spectra are adjusted to the same maximal intensity of the low-field shoulder. Fig. 1(b) shows that with increasing τ, the spectra change remarkably, such that at long τ, the maximal intensity is replaced by a hole. However, for the DCh sample (Fig. 1(a)), the spectra behavior is different – the hole does not appear and for the time delays 2τ larger than 2 μs, the spectra no longer tend to change.

The appearance of hole in ED EPR spectra of Fig. 1(b) can be easily explained basing on Eq. (1), as $\langle \sin^2(\xi_{(B-B_0)}/2)\rangle_{g(B)}$ is the largest for the field position B_0 corresponding to the EPR spectrum maximum. Fig. 1(c) presents spectra simulated using Eqs. (1) and (2). The initial EPR spectrum $E(0, B_0)$ at the zero time delay $\tau = 0$ (not shown) was calculated using g-tensor and hyperfine interaction parameters determined in a standard way from the CW EPR spectra. The microwave amplitude B_1 assessed from the experimental setup (see Experimental) is 0.56 mT; however, better agreement with experiment presented in Fig. 1(b) was found for $B_1 = 0.35$ mT (with corresponding enlarging t_p so that conserving the relation $\gamma t_p B_1 = \pi$); this discrepancy may arise

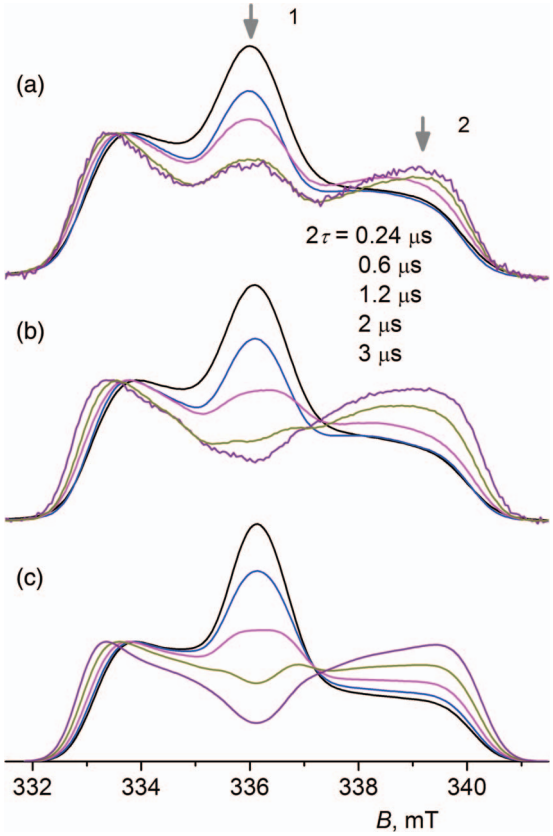

FIG. 1. ED EPR spectra experimentally obtained at 77 K or simulated for a concentration of 2 mol.%. (a) DCh in DPPC/DOPC bilayer. (b) 5-DSA in DPPC/DOPC bilayer. (c) Simulations using Eqs. (1) and (2) (see text). All spectra for convenience are adjusted to the same maximal intensity of the low-field shoulder. Arrows show field positions where echo decays were measured (see Fig. 2).

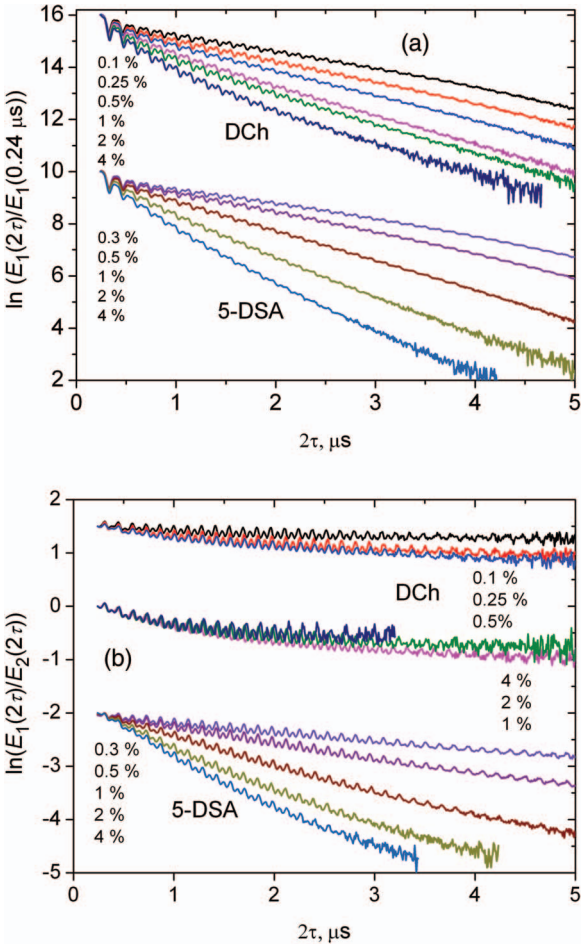

FIG. 2. (a) The semilogarithmic plot of ESE decay time traces obtained at position 1 in the EPR spectrum (see arrow in Fig. 1(a)), for different concentrations in mol.% of DCh and 5-DSA in the DPPC/DOPC bilayer. (b) The same for the ratios of ESE decay time traces obtained at positions 1 and 2. The curves are shifted along the vertical axis for convenience of presentation; concentrations are given in the vertical order corresponding to that of the curve tails.

from the non-ideality of the microwave pulse shape. The dimensionless parameter κ was set to 0.5. One can see that the calculated spectra resemble the experimental ones for the 5-DSA very closely (cf. Figs. 1(b) and 1(c)).

Note that Eq. (1) was obtained for a three-dimensional space distribution of spins, while in a planar lipid layer spin labels are expected to be distributed in 2 dimensions only. In that case the decay is expected to be proportional to $\exp(-(2\tau)^{2/3}$ const), as it could be easily assessed using the same approach as in Ref. 8. However, the ideal two-dimensional picture is destroyed by distribution of the spin label positions in the membrane and by interlayer interactions of spin labels, so that one should expect some intermediate picture between the cases of two and three dimensions. We suppose that the diminishing of κ parameter relative to the theoretical unity limit may appear also because of this deviation from the ideal three-dimensional case.

Another kind of experiment was measurement of the echo decays with increased τ and a fixed magnetic field. The echo decays were measured at the two field positions shown by arrows in Fig. 1(a), starting with the initial τ delay of 120 ns. The original time traces obtained for the 1st field position (i.e., at the maximum of the EPR spectrum) are presented in Fig. 2(a) in a semilogarithmic plot. Data are given for different molar ratios of DCh and 5-DSA in the DPPC/DOPC bilayer varying between 0.1 mol.% and 4 mol.%. One can see that the echo decay is strongly concentration-dependent. Small oscillations seen in the decay curves are induced by static electron-nuclear interactions with neighboring proton spins. This effect is called electron spin echo envelope modulation (ESEEM).[7] Note that since the oscillation is field-independent,[22] it may be considered as merely an insignificant multiplicative factor when studying the ED EPR spectra.

The ESE time traces in Fig. 2(a) show different behavior for the DCh sample and the 5-DSA sample used as a reference. This is especially clear when the time traces for the spectral positions 1 and 2 (see notations in Fig. 1(a)) are divided by each other – see semilogarithmic plot in Fig. 2(b). This division allows for extraction of the pure contribution of instantaneous diffusion, as all other contributions to the echo decay may be assumed to be field-independent (the influence of molecular motions is field-dependent too[22] but the temperature of measurements is too low for motions to be active); the rate of this contribution according to Eq. (1) is proportional to the difference $\langle \sin^2(\xi_{(B-B')}/2)\rangle_{g(B)} - \langle \sin^2(\xi_{(B-B'')}/2)\rangle_{g(B)}$, where B' and B'' are the B_0 values at the 1st and 2nd field

positions, respectively. One can see in Fig. 2(b) that a nearly linear time dependence and strong concentration dependence for 5-DSA are replaced by an extended time dependence and weak concentration dependence for DCh attaining even a "reverse" character of dependence on concentration when the latter is higher than 1%.

DISCUSSION

Data in Figs. 1 and 2 can be readily explained by assuming that for DCh samples, the value of $\langle \sin^2(\xi_{(B-B_0)}/2)\rangle_{g(B)}$ becomes nearly the same for all spectral positions B_0. This closeness may appear if the bilayers consist of domains with equally oriented DCh molecules. The EPR spectra for these domains must contain three equally spaced lines of the same amplitude, like in a single crystal. For these "intrinsic" spectra, the total ED EPR line shape is not expected to provide τ dependence, because all three lines are equally suppressed by the instantaneous diffusion mechanism. Note that as different domains have different orientations, the resulting total spectrum is the same as in the case of random label orientations. The size of domains in this interpretation is not determined; it may vary starting from several nanometers. Also, it could be a scenario when orientation of the DChol molecules changes slowly and continuously when going around the circumference of the vesicle, without forming domains at all.

Of course, the τ-independence is expected for only the ideal case when the mutual molecular orientations are perfectly the same and when magnetic dipole-dipolar interactions between electron spins of neighboring domains (if they exist) may be neglected. Otherwise, one would observe a mixture of the τ-dependence for the domain model and for the model of random molecular orientations that just what is seen for the DCh ED EPR spectra in Fig. 1(a).

It is important to note that CW EPR spectra (see above) and the time traces of echo decays in Fig. 2(a) provide evidence that formation of domains is not accompanied by the aggregation of DCh molecules. Indeed, aggregation would immediately manifest itself in a severe broadening of the EPR lineshape and in accelerating echo decays for the DCh sample (as compared with the reference 5-DSA sample), which is not observed in our case. So within the suggested interpretation the DCh molecules remain spatially diluted, and the term "domain" refers only to the mutual molecular orientation.

The correlation of molecular orientations can be readily explained taking into account that DCh molecules because of their flat structure can correspondingly organize the immediate lipid surrounding in the bilayer, and this additional molecular order can be translated to other neighboring lipids. So long-range interaction between DCh molecules can appear which is mediated by surrounding lipid molecules. 5-DSA molecules in the reference system have no flat structure and therefore lack this possibility of creating the order of that kind in the immediate lipid surrounding.

As the DCh sample and reference 5-DSA sample manifest different temporal behavior even at concentration as small as 0.5 mol.% (see Fig. 2(b)), the concentration threshold for the domain formation lies below this value. Also, we note that formation of these "orientational domains" can serve as precursors for the raft formation.[1–5]

The most important point in further studies could be the elucidation of the size of these domains of similarly oriented cholesterol molecules.

ACKNOWLEDGMENTS

Authors are thankful to Nikolay Isaev for useful discussion and assistance in the beginning of these experiments. This work was supported by RFBR Grant No. 12-03-00192-a.

[1]D. Lingwood and K. Simons, Science **327**, 46–50 (2010).
[2]I. V. Ionova, V. A. Livshits, and D. Marsh, Biophys. J. **102**, 1856–1865 (2012).
[3]J. R. Silvius, Biochim. Biophys. Acta **1610**, 174–183 (2003).
[4]K. J. Fritzsching, J. Kim, and G. P. Holland, Biochim. Biophys. Acta **1828**, 1889–1898 (2013).
[5]I. Levental, M. Grzybek, and K. Simons, Biochemistry **49**, 6305–6316 (2010).
[6]T. T. Mills, S. Tristram-Nagle, F. A. Heberle, N. F. Morales, J. Zhao, J. Wu, G. E. S. Toombes, J. F. Nagle, and G. W. Feigenson, Biophys. J. **95**, 682–690 (2008).
[7]A. Schweiger and G. Jeschke, *Principles of Pulse Electron Paramagnetic Resonance* (Oxford University Press, Oxford, 2001).
[8]J. R. Klauder and P. W. Anderson, Phys. Rev. **125**, 912–932 (1962).
[9]K. M. Salikhov, S. A. Dzuba, and A. M. Raitsimring, J. Magn. Reson. **42**, 255–276 (1981).
[10]R. I. Samoilova, A. M. Raitsimring, and Y. D. Tsvetkov, Radiat. Phys. Chem. **15**, 553–559 (1980).
[11]B. Rakvin, N. Maltar-Strmecki, and K. Nakagawa, Radiat. Measur. **42**, 1469–1474 (2007).
[12]M. Marrale, M. Brai, A. Barbon, and M. Brustolon, Radiat. Res. **171**, 349–359 (2009).
[13]D. A. Erilov, R. Bartucci, R. Guzzi, D. Marsh, S. A. Dzuba, and L. Sportelli, J. Phys. Chem. B. **108**, 4501–4507 (2004).
[14]R. Dastvan, B. E. Bode, M. P. R. Karuppiah, A. Marko, S. Lyubenova, H. Schwalbe, and T. F. Prisner, J. Phys. Chem. B **114**, 13507–13516 (2010).
[15]S. K. Hoffmann, S. Lijewski, J. Goslar, and V. A. Ulanov, J. Magn. Reson. **202**, 14–23 (2010).
[16]A. M. Tyryshkin, S. A. Lyon, A. V. Astashkin, and A. M. Raitsimring, Phys. Rev. B **68**, 193207 (2003).
[17]A. Ferretti, M. Fanciulli, A. Ponti, and A. Schweiger, Phys. Rev. B **72**, 235201 (2005).
[18]A. Grammenos, A. Mouithys-Mickalad, P. H. Guelluy, M. Lismont, G. Piel, and M. Hoebeke, Biochem. Biophys. Res. Commun. **398**, 350 (2010).
[19]J. A. Williams, C. D. Wassall, M. D. Kemple, and S. R. Wassall, J. Membr. Biol. **246**, 689–696 (2013).
[20]F. M. Megli, E. Conte, and T. Ishikawa, Biochim. Biophys. Acta **1808**, 2267–2274 (2011).
[21]E. D. Walter, K. B. Sebby, R. J. Usselman, D. J. Singel, and M. J. Cloninger, J. Phys. Chem. B **109**, 21532–21538 (2005).
[22]N. P. Isaev and S. A. Dzuba, J. Phys. Chem. B. **112**, 13285–13291 (2008).